

Examination and visualization of the simplifying assumption for vine copulas in three dimensions

Matthias Killiches*, Daniel Kraus† and Claudia Czado‡

April 30, 2022

Abstract

Vine copulas are a highly flexible class of dependence models, which are based on the decomposition of the density into bivariate building blocks. For applications one usually makes the simplifying assumption that copulas of conditional distributions are independent of the variables they are conditioned on. However, this assumption has been criticized for being too restrictive. We examine both simplified and non-simplified vines in three dimensions and try to find out conceptual differences. For this purpose we show and compare contour surfaces of three-dimensional vine copula models, which prove to be much more informative than the contour lines of the bivariate marginals. In addition to a variety of constructed examples, we also investigate a three-dimensional subset of the well-known uranium data set.

Keywords: Vine copulas, simplifying assumption, visualization, contour surfaces.

1 Introduction

Dependence modeling has become a growing research area of high interest in the last decades. In finance, regulatory requirements like Basel III ([Basel Committee on Banking Supervision \(2009\)](#)) and Solvency II ([European Parliament and European Council \(2009\)](#)) have raised the need for sophisticated risk assessment making a proper understanding of the interdependencies between different quantities inevitable. For hydrological applications the dependence between rainfall, wind speed and other parameters is crucial for setting up appropriate models. Basically, dependence plays a role whenever there is more than one source of randomness. Among dependence models copulas have taken a prominent role since they allow for a separate modeling of marginal distributions and dependence structure ([Sklar \(1959\)](#)). A special class of copulas are so-called *vine copulas*, also known as *pair-copula constructions*, which are based on a decomposition of the joint density into bivariate building blocks. Since the publication of the seminal papers by [Bedford and Cooke \(2002\)](#) and [Aas et al. \(2009\)](#), these copulas have gained more and more popularity due to their flexibility and numerical applicability. When working with vines one often makes the *simplifying assumption* that copulas of conditional distributions are independent of the values of the variables they are conditioned on. Although enabling estimation and inference even in high dimensions, this assumption has also been criticized (e.g. [Acar et al. \(2012\)](#), [Spanhel and Kurz \(2015\)](#)). Our goal is to shed some light on the implications of the simplifying assumption by visualizing the densities of simplified and non-simplified models. For this purpose, we concentrate on the three-dimensional case. This

*Zentrum Mathematik, Technische Universität München, Boltzmannstraße 3, 85748 Garching, Germany. Email: matthias.killiches@tum.de.

†Zentrum Mathematik, Technische Universität München, Boltzmannstraße 3, 85748 Garching, Germany. Email: daniel.kraus@tum.de.

‡Zentrum Mathematik, Technische Universität München, Boltzmannstraße 3, 85748 Garching, Germany. Email: cczado@ma.tum.de.

has the advantage that the corresponding pair-copula construction contains only one copula describing the dependence between conditional variables, making the interpretation of the results easier. Further, it is still possible to visualize three-dimensional densities by plotting their contour surfaces. We will see that these plots contain much more information than the bivariate contour lines of the three two-dimensional margins.

The paper is organized as follows: In [Section 2](#) we provide an introduction to vine copulas and a formal definition of the simplifying assumption. While we show visualizations of simplified vines in [Section 3](#), [Section 4](#) contains three-dimensional plots of non-simplified vines. Further we present applications to simulated and real data ([Section 5](#)). The paper concludes with [Section 6](#). In addition to the paper, we provide a web-application (implemented using Shiny by RStudio) for generating three-dimensional vine copula objects (<https://vinecopula.shinyapps.io/Vine3DPlot>).

2 Vine copulas and the simplifying assumption

Since the seminal work of Sklar has been published ([Sklar \(1959\)](#)) the concept of *copulas* has become more and more popular in statistical modeling. Copulas are d -dimensional distribution functions on the hypercube $[0, 1]^d$ with uniformly distributed margins. The following relationship proven in *Sklar's Theorem* makes copulas extremely useful for statistical applications: Let $F: \mathbb{R}^d \rightarrow [0, 1]$ be the joint distribution function of a d -dimensional random variable $(X_1, \dots, X_d)'$ with univariate marginal distribution functions F_j , $j = 1, \dots, d$. Then, there exists a copula $C: [0, 1]^d \rightarrow [0, 1]$ such that

$$F(x_1, \dots, x_d) = C(F_1(x_1), \dots, F_d(x_d)). \quad (2.1)$$

This copula C is unique if all X_j are continuous. If additionally the so-called *copula density*

$$c(u_1, \dots, u_d) := \frac{\partial^d}{\partial u_1 \dots \partial u_d} C(u_1, \dots, u_d)$$

exists, we have

$$f(x_1, \dots, x_d) = c(F_1(x_1), \dots, F_d(x_d)) f_1(x_1) \dots f_d(x_d), \quad (2.2)$$

where f_j are the marginal densities. Conversely, one can specify a multivariate distribution based on a copula and d marginal distributions with the help of [Equation \(2.1\)](#) and [Equation \(2.2\)](#), respectively. This means that marginals and dependence structure can be modeled separately. [Nelsen \(2006\)](#) and [Joe \(1997\)](#) provide an extensive treatment of theoretical and practical aspects of copulas.

For modeling purposes many copula classes have been developed, e.g. elliptical, Archimedean and extreme-value copulas. Usually the copula families in these classes are determined by a small number of parameters such that they are rather inflexible in high dimensions. This lack of flexibility has been overcome by *vine copulas*. The concept of constructing copula densities using a combination of only bivariate building blocks was introduced in [Bedford and Cooke \(2002\)](#). Based on this work, [Aas et al. \(2009\)](#) developed statistical inference methods using these vine copulas or *pair-copula constructions* (PCCs). This class of copulas has been a frequent subject of recent research. [Dißmann et al. \(2013\)](#) present a sequential estimation method for vine copulas. A particular class of vine models is used for quantile regression in [Kraus and Czado \(2015\)](#) and the dependence of finite block maxima of vines is investigated in [Killiches and Czado \(2015\)](#). To extend the approach to non-continuous and non-parametric models [Panagiotelis et al. \(2012\)](#) study the application to discrete data and [Nagler and Czado \(2015\)](#) provide a kernel density based estimation method for vines. Further, there is a multitude of real data applications, especially in the context of finance (e.g. [Brechmann et al.](#)

(2014), Maya et al. (2015) and Brechmann and Czado (2013)). Extended models for describing geo-spatial dependence are introduced in Erhardt et al. (2015a) and Erhardt et al. (2015b). Vine copulas are particularly interesting for researchers and practitioners from all fields due to the R package `VineCopula` (Schepsmeier et al. (2015)), where algorithms for estimation, simulation and model diagnostics are implemented.

Since we will only consider three-dimensional examples in this paper, we introduce the concept of vine copulas in $d = 3$ dimensions. For a general introduction to vine copulas we refer to Aas et al. (2009) and Stöber and Czado (2012). Using Sklar's Theorem for densities (Equation (2.2)) and the fact that the one-dimensional marginals of a copula are uniformly distributed, i.e. $c_j(u_j) = 1$ for any $u_j \in [0, 1]$, we can decompose the copula density c of a random vector $\mathbf{U} = (U_1, U_2, U_3)'$ with uniformly distributed margins U_j as follows:

$$\begin{aligned} c(u_1, u_2, u_3) &= c_{13|2}(u_1, u_3|u_2) c_2(u_2) \\ &\stackrel{\text{Sklar}}{=} c_{13;2}(C_{1|2}(u_1|u_2), C_{3|2}(u_3|u_2); u_2) c_{1|2}(u_1|u_2) c_{2|3}(u_2|u_3) \\ &= c_{13;2}(C_{1|2}(u_1|u_2), C_{3|2}(u_3|u_2); u_2) c_{12}(u_1, u_2) c_{23}(u_2, u_3), \end{aligned} \quad (2.3)$$

where $c_{13|2}(\cdot, \cdot | u_2)$ is the density of the conditional distribution of $(U_1, U_3) | U_2 = u_2$, whereas $c_{13;2}(\cdot, \cdot; u_2)$ is the copula density associated with the conditional distribution of $(U_1, U_3) | U_2 = u_2$. The distribution function of the conditional distribution of U_j given $U_2 = u_2$ is denoted by $C_{j|2}(\cdot | u_2)$, $j = 1, 3$. It can be obtained by partial differentiation (Joe (1997)): $C_{1|2}(u_1|u_2) = \frac{\partial}{\partial u_2} C_{12}(u_1, u_2)$ and $C_{3|2}(u_3|u_2) = \frac{\partial}{\partial u_2} C_{23}(u_2, u_3)$. Hence, we can describe the entire copula density c by specifying only three bivariate copulas.

Note that it would also have been possible to choose U_1 or U_3 as conditioning variable. Then, we would have ended up with

$$c(u_1, u_2, u_3) = c_{23;1}(C_{2|1}(u_2|u_1), C_{3|1}(u_3|u_1); u_1) c_{12}(u_1, u_2) c_{13}(u_1, u_3)$$

or

$$c(u_1, u_2, u_3) = c_{12;3}(C_{1|3}(u_1|u_3), C_{2|3}(u_2|u_3); u_3) c_{13}(u_1, u_3) c_{23}(u_2, u_3),$$

respectively. However, for our purpose all three structures are equivalent since they can be obtained by relabeling. Therefore, throughout the paper we will always use the decomposition from Equation (2.3). Here, the bivariate marginals c_{12} and c_{23} are explicitly specified. The third bivariate marginal c_{13} is implicitly defined and can be obtained via one-dimensional integration:

$$c_{13}(u_1, u_3) = \int_0^1 c(u_1, v, u_3) dv. \quad (2.4)$$

In general the bivariate copula density function $c_{13;2}(\cdot, \cdot; u_2)$ depends on the value of u_2 . Yet, when it comes to modeling, one often makes the so-called *simplifying assumption* that $c_{13;2}$ does not depend on u_2 , i.e.

$$c_{13;2}(u_1, u_3; u_2) = c_{13;2}(u_1, u_3)$$

for all $u_1, u_2, u_3 \in [0, 1]$. To enable fast and robust inference this assumption is made in a multitude of cases. Nevertheless, there has also been research on *non-simplified vines* and the question when the simplifying assumption is justified. Stöber et al. (2013) investigate which multivariate copula models can be decomposed into a simplified vine copula. While Haff et al. (2010) come to the conclusion that simplified vines are “a rather good solution, even when the simplifying assumption is far from being fulfilled by the actual model”, Acar et al. (2012) criticize this statement as being too optimistic and show cases where non-simplified vines are needed. In particular, they look at a three-dimensional subset of the uranium data set from the R package `copula` (Hofert et al. (2015)) and decide that it cannot be modeled by simplified vine. Killiches et al. (2015) develop a test for the simplifying assumption and

apply it to the same data set obtaining similar results. In the test they use the R package `gamCopula` (Vatter (2015)), which can be used for the estimation of non-simplified vine copula models with the help of generalized additive models (Vatter and Nagler (2015)). A critical view on the simplifying assumption is presented in Spanhel and Kurz (2015), where the focus lies on possible misspecifications of simplified vines when the underlying true model is non-simplified. This paper contributes to this discussion by focusing the visual implications of the simplifying assumption.

In the following sections we will use the parametric bivariate copula families implemented in `VineCopula` as building blocks. This includes Gaussian (\mathcal{N}), t (t), Clayton (\mathcal{C}), Gumbel (\mathcal{G}), Frank (\mathcal{F}), Joe (\mathcal{J}), Clayton-Gumbel (BB1), Joe-Gumbel (BB6), Joe-Clayton (BB7), Joe-Frank (BB8), Tawn type 1 ($\mathcal{T}_{(1)}$) and Tawn type 2 ($\mathcal{T}_{(2)}$) copulas as well as their survival versions and rotations by 90 degrees and 270 degrees (indicated by the superscripts 180, 90 or 270, respectively). The densities of the survival and rotated versions of a bivariate copula density c can be obtained in the following way:

$$\begin{aligned} c^{90}(u_1, u_2) &= c(1 - u_2, u_1), \\ c^{180}(u_1, u_2) &= c(1 - u_1, 1 - u_2), \\ c^{270}(u_1, u_2) &= c(u_2, 1 - u_1). \end{aligned}$$

When we specify a pair-copula, we state the family and the corresponding parameters. For example, a t copula with association parameter $\rho = 0.5$ and $\nu = 3$ degrees of freedom is denoted by $t(0.5, 3)$ and $\mathcal{T}_{(2)}^{270}(-3, 0.6)$ stands for a Tawn type 2 copula rotated by 270 degrees with first parameter -3 and second parameter 0.6 .

The space of admissible parameters depends on the copula family. For example, whereas the parameter space of a t copula is $(-1, 1) \times (2, \infty)$, the one of a Frank copula is given by $\mathbb{R} \setminus \{0\}$. Since we still want to compare different copula families we transform the parameters to the same scale using Kendall's τ as a measure for the strength of dependence. Kendall's τ between two variables X and Y is defined as follows: Let $(X_1, Y_1)'$ and $(X_2, Y_2)'$ be two independent and identically distributed copies of $(X, Y)'$. Then, τ is defined as the probability that $(X_1, Y_1)'$ and $(X_2, Y_2)'$ are concordant minus the probability that they are discordant, i.e.

$$\tau = \mathbb{P}((X_1 - X_2)(Y_1 - Y_2) > 0) - \mathbb{P}((X_1 - X_2)(Y_1 - Y_2) < 0).$$

Obviously, τ can only take values between -1 and 1 , where the boundary points of the interval are only taken if X is strictly decreasing or increasing function of Y , respectively. If the copula C of a bivariate distribution is known, then (as proven in Nelsen (2006)) the corresponding Kendall's τ value can also be calculated via

$$\tau = 4 \int_{[0,1]^2} C(u_1, u_2) dC(u_1, u_2) - 1.$$

3 Visualization of simplified vines

The contour of a density $f: \mathbb{R}^d \rightarrow [0, \infty)$ corresponding to a level $y \in (0, \infty)$ is the set $\{\mathbf{z} \in \mathbb{R}^d \mid f(\mathbf{z}) = y\}$ of all points in \mathbb{R}^d that are assigned the same density value y . For bivariate densities, plots of contour lines are well-known; in three dimensions this concept is extended to contour surfaces. In this section we present contour plots of various simplified three-dimensional vine copula densities, ranging from very simple models as for example a Gaussian vine to more complex scenarios. The main goal is to get a feeling for how simplified vines look like in order to properly compare them to non-simplified vines. Additionally to the three-dimensional contour surfaces plotted from three different angles we present the contour

sc.	p.	copula c_{12}				copula c_{23}				copula $c_{13;2}$			
		family	$\theta_{12}^{(1)}$	$\theta_{12}^{(2)}$	τ_{12}	family	$\theta_{23}^{(1)}$	$\theta_{23}^{(2)}$	τ_{23}	family	$\theta_{13;2}^{(1)}$	$\theta_{13;2}^{(2)}$	$\tau_{13;2}$
1	5	\mathcal{N}	0.6	–	0.41	\mathcal{N}	0.7	–	0.49	\mathcal{N}	0.5	–	0.33
2	6	t	0.6	3	0.41	t	0.7	3	0.49	t	0.5	4	0.33
3	7	t	0.6	3	0.41	t	0.7	7	0.49	t	0.5	5	0.33
4	8	\mathcal{C}	2	–	0.50	\mathcal{C}	2	–	0.50	\mathcal{C}	0.67	–	0.25
5	8	\mathcal{C}^{90}	–2	–	–0.50	\mathcal{C}	2	–	0.50	\mathcal{C}	1.5	–	0.43
6	9	\mathcal{F}	7	–	0.56	\mathcal{G}	2	–	0.50	\mathcal{N}	–0.7	–	–0.49
7	9	$\mathcal{T}_{(1)}$	3	0.3	0.25	\mathcal{J}^{270}	–2	–	–0.36	BB1	2	1.5	0.67

Table 1: Simplified vine copula specifications considered in [Section 3](#).

lines of the two-dimensional marginals c_{12} , c_{23} and c_{13} . While c_{12} and c_{23} are explicitly specified in the vine copula construction, the margin c_{13} has to be calculated by integrating c_{123} with respect to u_2 , either analytically (when possible) or numerically (cf. [Equation \(2.4\)](#)).

For all two- and three-dimensional contour plots we set the univariate marginals to a standard normal distribution, i.e. we consider the random vector $\mathbf{Z} = (Z_1, Z_2, Z_3)'$, where $Z_j := \Phi^{-1}(U_j)$, $j = 1, 2, 3$, with Φ denoting the standard normal distribution function. This is done because on the uniform scale copula densities would be difficult to interpret and hardly comparable with each other. Further, in this way a Gaussian copula results in a Gaussian distribution so that all examples can be seen in comparison to this well-known case.

For interested readers we refer to our web-application (<https://vinecopula.shinyapps.io/Vine3DPlot>), where three-dimensional vine copula objects can be generated and rotated at one’s convenience. This might be interesting if one wants to look at the contour plots of our scenarios from another angle or if one is interested in visualizing own examples.

In [Section 3](#) we will consider the simplified vine copula specifications from [Table 1](#). For each scenario the three pair-copulas are specified by their families and parameter(s). Further, we state the corresponding Kendall’s τ value in order to facilitate comparability.

3.1 Simplified vines with elliptical pair-copulas

Gaussian copula

The first scenario we consider is a Gaussian copula. Among others, [Stöber et al. \(2013\)](#) show that every Gaussian copula can be represented as a simplified *Gaussian vine* (i.e. all pair-copulas are Gaussian) and vice versa. We specify the pair-copulas of the vine as follows: c_{12} is a bivariate Gaussian copula with parameter $\rho_{12} = 0.6$ (i.e. $\tau_{12} = 0.41$), c_{23} is a Gaussian copula with $\rho_{23} = 0.7$ ($\tau_{23} = 0.49$) and $c_{13;2}$ is a Gaussian copula with $\rho_{13;2} = 0.5$ ($\tau_{13;2} = 0.33$). This specification, which can be found in [Table 1](#) (Scenario 1), directly implies that c_{13} is a Gaussian copula with $\rho_{13} = 0.71$ ($\tau_{13} = 0.50$), see for example [Kurowicka and Cooke \(2006\)](#). The resulting ellipsoids displayed from three viewpoints in the top row of [Figure 1](#) are the natural extension of the well-known ellipse-shaped contour plots of bivariate normal distributions. We choose the levels for the contour plots such that the four contour surfaces are representative for the entire density. For the remainder of this paper these levels are fixed with values 0.015, 0.035, 0.075 and 0.11 (from outer to inner surface). The contour plots of the two-dimensional margins in the top row of [Figure 2](#) are those of bivariate normal distributions.

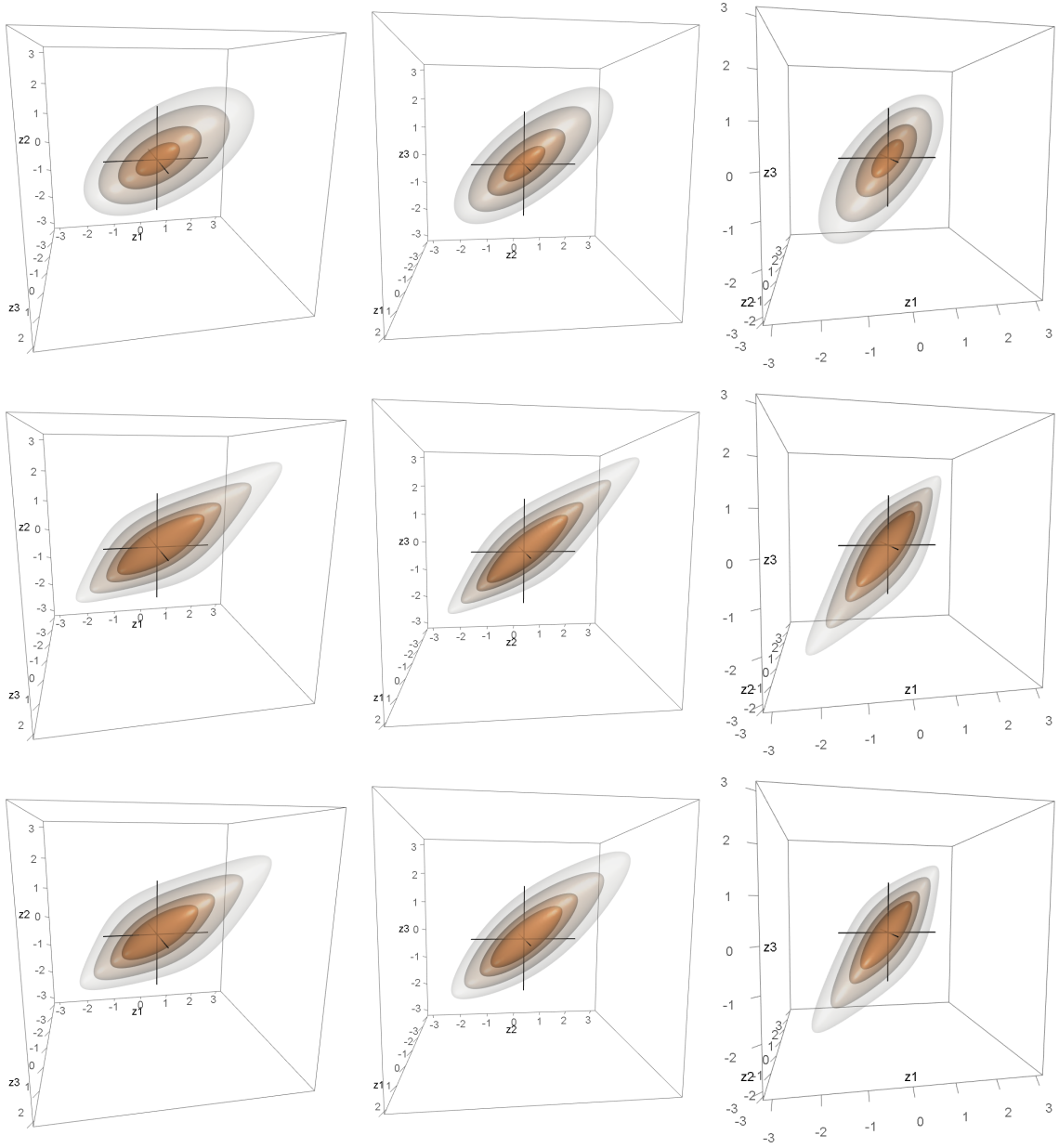


Figure 1: Top row (Scenario 1): Contours of the vine specified by c_{12} : $\mathcal{N}(0.6)$, c_{23} : $\mathcal{N}(0.7)$, $c_{13;2}$: $\mathcal{N}(0.5)$.
Middle row (Scenario 2): Contours of the vine specified by c_{12} : $t(0.6, 3)$, c_{23} : $t(0.7, 3)$, $c_{13;2}$: $t(0.5, 4)$.
Bottom row (Scenario 3): Contours of the vine specified by c_{12} : $t(0.6, 3)$, c_{23} : $t(0.7, 7)$, $c_{13;2}$: $t(0.5, 5)$.

t copula

As a second example we consider another member of the family of elliptical copulas, the three-dimensional t copula with ν degrees of freedom. Recall (e.g. from [Demarta and McNeil \(2005\)](#)) that the Gaussian copula is the limiting case of the t copula as $\nu \rightarrow \infty$ and that the t copula exhibits a positive upper and lower tail dependence being more pronounced for small ν . We examine a three-dimensional t copula with $\nu = 3$ degrees of freedom and the same association parameters as in the previous example of the Gaussian copula. We know that the vine decomposition of a t copula with ν degrees of freedom results in the unconditional pair-copulas having ν degrees of freedom and the conditional pair-copula having $\nu + 1$ degrees of freedom ([Stöber et al. \(2013\)](#)). The resulting specification can be found in [Table 1](#) as

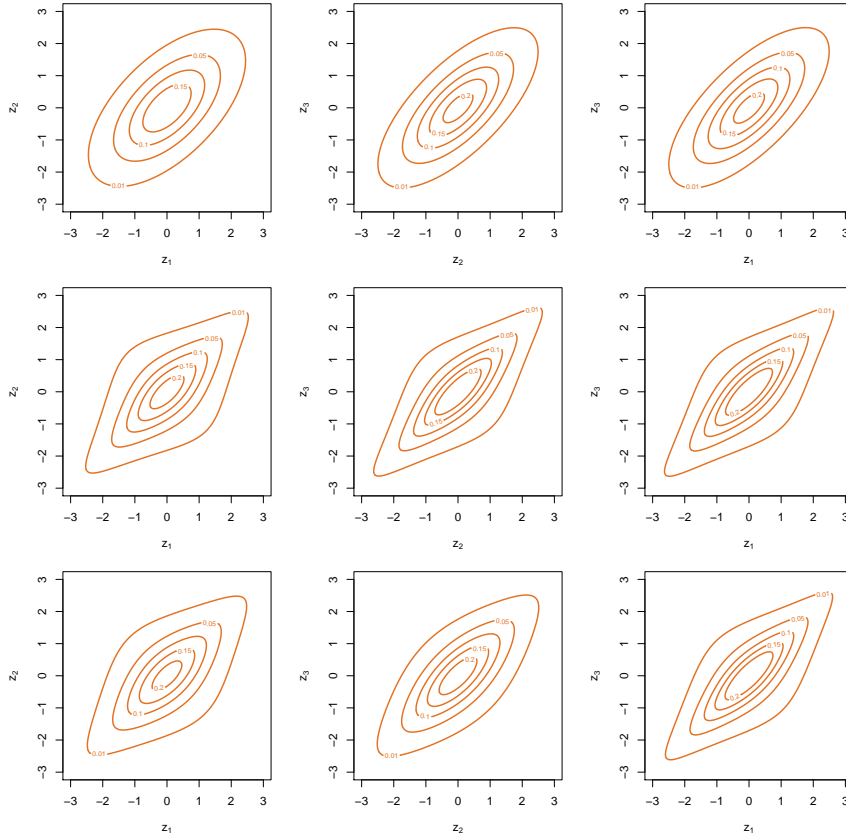


Figure 2: Contour plots of the bivariate margins c_{12} , c_{23} and c_{13} . Top row: Scenario 1. Middle row: Scenario 2. Bottom row: Scenario 3.

Scenario 2. The three-dimensional contours of the t copula in [Figure 1](#) (middle row) exhibit the typical diamond shape we know from bivariate t copula contours (see [Figure 2](#), middle row). Comparing these contours to those of the Gaussian copula we see that the t copula has significantly more weight in the tails of the distribution originating from the positive tail dependence.

t vine

In contrast to a t copula, where only one degree of freedom can be specified, all pair-copulas of a t vine may have different degrees of freedom. This might be useful when modeling the dependencies of financial returns which tend to be t distributed, where, however, each pair of variables might have a different strength of tail dependence. In Scenario 3 (cf. [Table 1](#)), we consider a t vine with the same association parameters as above but changed degrees of freedom: $\nu_{12} = 3$, $\nu_{23} = 7$ and $\nu_{13;2} = 5$. This case is illustrated in the bottom row of [Figure 1](#): We can see that the tail dependence of the pairs is different, which is also visible in the bivariate contours in [Figure 2](#) (bottom row). Although the visual difference between the plots of the middle and bottom row of [Figure 1](#) does not seem to be very pronounced, the differences in the tails are substantial, influencing the assessment of extreme events considerably.

In all three examples from this section, the contour plots of the bivariate margins already give the beholder a good impression of what the three-dimensional object looks like. It turns out that this property can be observed for all simplified vines we will consider.

3.2 Simplified vine with Archimedean pair-copulas

Clayton copula

A well-known representative of the class of Archimedean copulas is the Clayton copula. It is a one-parametric family with lower tail dependence. The Clayton copula is the copula underlying the multivariate Pareto distribution and is the only Archimedean copula that can be represented as a simplified vine as stated in [Stöber et al. \(2013\)](#). It is easy to see that the bivariate margins of a three-dimensional Clayton copula with parameter θ are bivariate Clayton copulas with parameter θ , see for example [Kraus and Czado \(2015\)](#), Appendix B. There it is also shown that the copula of the conditioned variables (in our decomposition $c_{13;2}$) again is a Clayton copula, in this case with parameter $\theta/(\theta + 1)$. Hence, in order to obtain a three-dimensional Clayton copula with parameter $\theta = 2$ we specify a vine as described in Scenario 4 of [Table 1](#). [Figure 3](#) (top row) displays the contours of the resulting copula, the strong lower tail dependence is clearly visible. As already stated, the bivariate margin c_{13} is also a Clayton copula with parameter 2 and therefore all contour plots of the margins in the top row of [Figure 4](#) are identical.

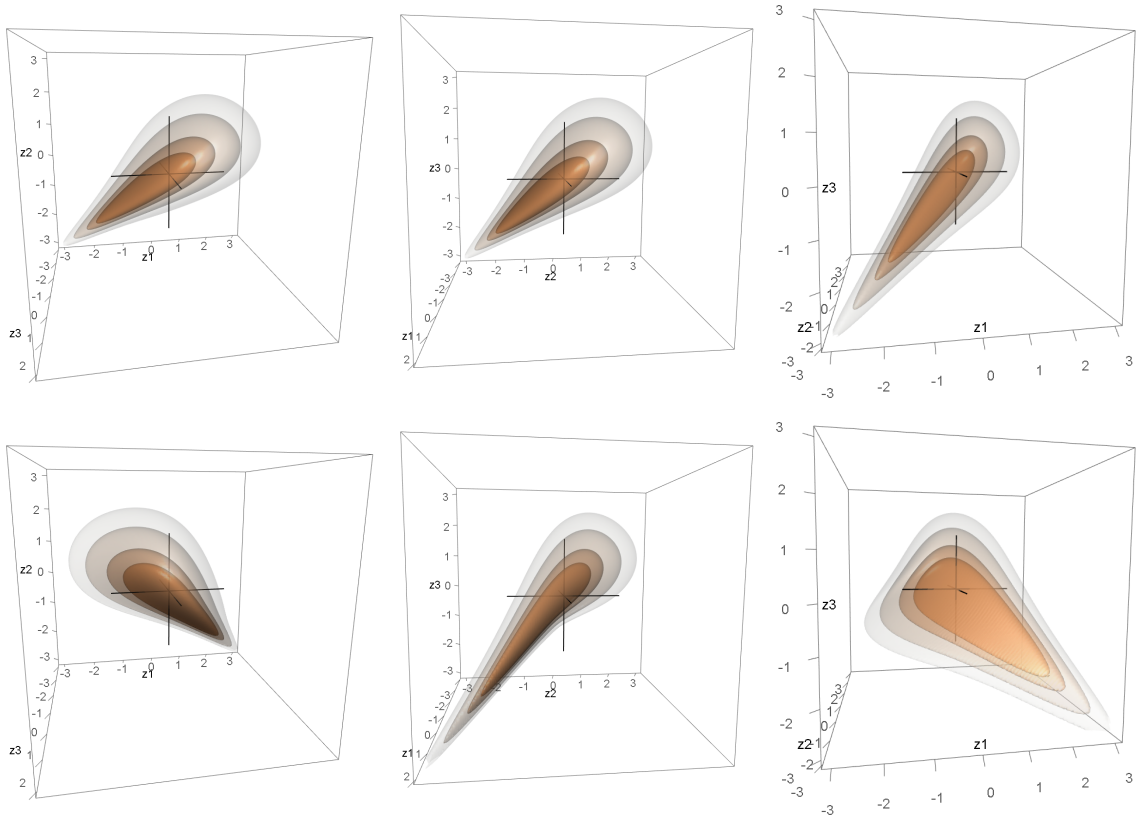


Figure 3: Top row (Scenario 4): Contours of the vine specified by $c_{12}: \mathcal{C}(2)$, $c_{23}: \mathcal{C}(2)$, $c_{13;2}: \mathcal{C}(0.67)$.

Bottom row (Scenario 5): Contours of the vine specified by $c_{12}: \mathcal{C}^{90}(-2)$, $c_{23}: \mathcal{C}(2)$, $c_{13;2}: \mathcal{C}(1.5)$.

Clayton vine

While being a useful tool in two dimensions to model pairs with lower tail dependence, the Clayton copula can be criticized to be too inflexible in higher dimensions because only one parameter is used to model the dependence between several variables. Further, the assumption that all bivariate margins have the same distribution is too strict in the majority of applications. With a *Clayton vine* we gain the flexibility of specifying each pair-copula individually as a bivariate Clayton copula with different parameters. In the example shown in [Figure 3](#) (bottom row) we specify the three pair-copulas to be (90 degree rotated) Clayton

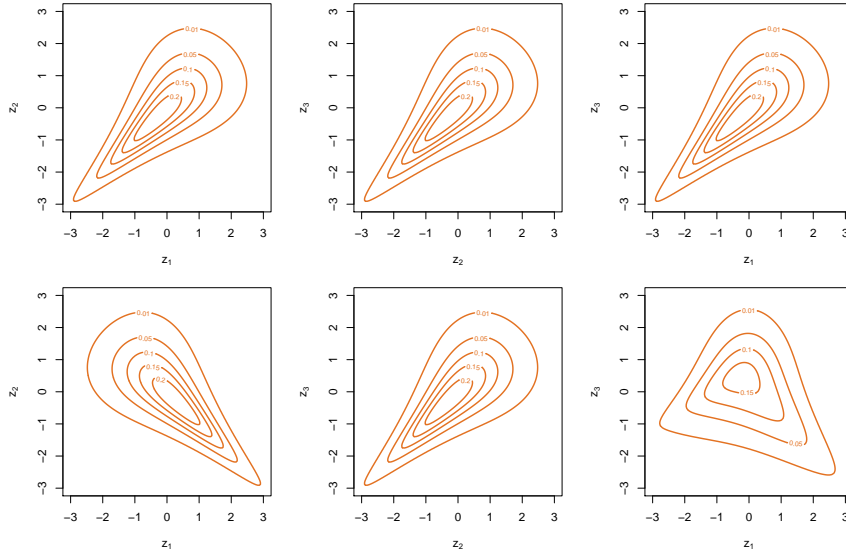


Figure 4: Contour plots of the bivariate margins c_{12} , c_{23} and c_{13} . Top row: Scenario 4. Bottom row: Scenario 5.

with parameters $\theta_{12} = -2$, $\theta_{23} = 2$ and $\theta_{13;2} = 1.5$ (see Scenario 5 in Table 1), illustrating that the Clayton vine allows us to model positive as well as negative dependencies with different strengths of dependence. The resulting three-dimensional density, whose contours are depicted in the bottom row of Figure 3, clearly deviates from the Clayton copula. Especially the dependence between the first and third variable is far from any standard parametric copula family (see also the numerically derived contours of c_{13} in Figure 4, bottom right panel).

For the two considered Clayton examples we also observe that the shape of the contours of the three-dimensional density is already being anticipated quite well by the two dimensional marginal plots.

3.3 Mixed simplified vine specifications

Mixed vine 1

Up to now, we only considered vines where all pair-copulas belonged to the same family of parametric copulas. Of course, one of the main advantages of vine copulas is that one can specify each pair to be from a different copula family with its own parameter(s). The resulting model class is very flexible and able to describe many different kinds of dependencies. As an example for this, we present Scenario 6 (Table 1): c_{12} is a bivariate Frank copula with parameter $\theta_{12} = 7$, c_{23} is a Gumbel copula with $\theta_{23} = 2$ and $c_{13;2}$ is a Gaussian copula with $\rho_{13;2} = -0.7$. In the resulting contour plots of Figure 5 (top row) one can clearly see the shapes of the Frank and the Gumbel copula in the left and the middle plot, respectively. Although the dependency of each pair-copula is fairly strong, we observe rather weak dependence for c_{13} . The negative conditional dependence seems to cancel out with the positive dependencies implied by c_{12} and c_{23} (compare Figure 6, top row).

Mixed vine 2

We consider a second example of a mixed vine (Scenario 7 from Table 1) with the following specifications: c_{12} is a Tawn Type 1 copula with parameters $\theta_{12} = (3, 0.3)'$, c_{23} is a Joe copula rotated by 270 degrees with $\theta_{23} = -2$ and $c_{13;2}$ is a BB1 copula with $\theta_{13;2} = (2, 1.5)'$. The shape of the resulting contours in the bottom row of Figure 5 appears to be very non-standard. Especially the dependence between the first and third marginals is quite contorted. The dependence structure of the copula of the conditioned variables (BB1) cannot be detected

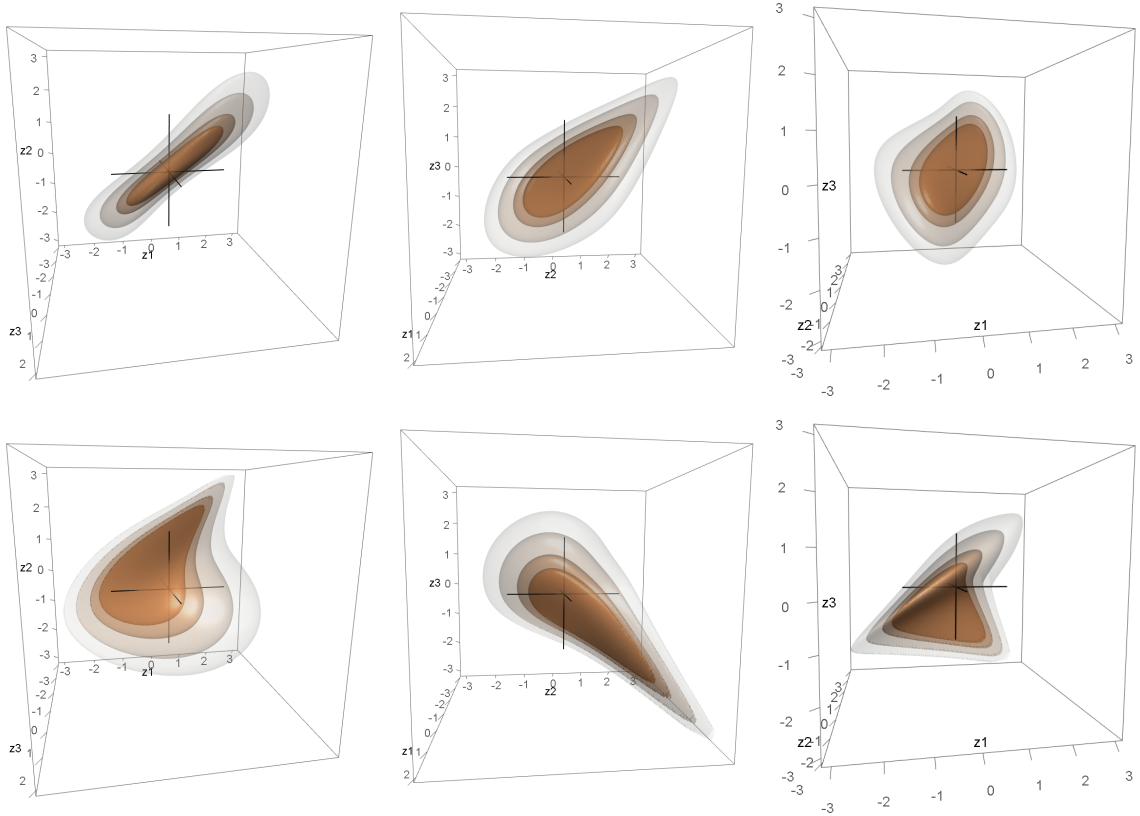


Figure 5: Top row (Scenario 6): Contours of the vine specified by c_{12} : $\mathcal{F}(7)$, c_{23} : $\mathcal{G}(2)$, $c_{13;2}$: $\mathcal{N}(-0.7)$.
 Bottom row (Scenario 7): Contours of the vine specified by c_{12} : $\mathcal{T}_{(1)}(3, 0.3)$, c_{23} : $\mathcal{J}^{270}(-2)$, $c_{13;2}$: $\text{BB1}(2, 1.5)$.

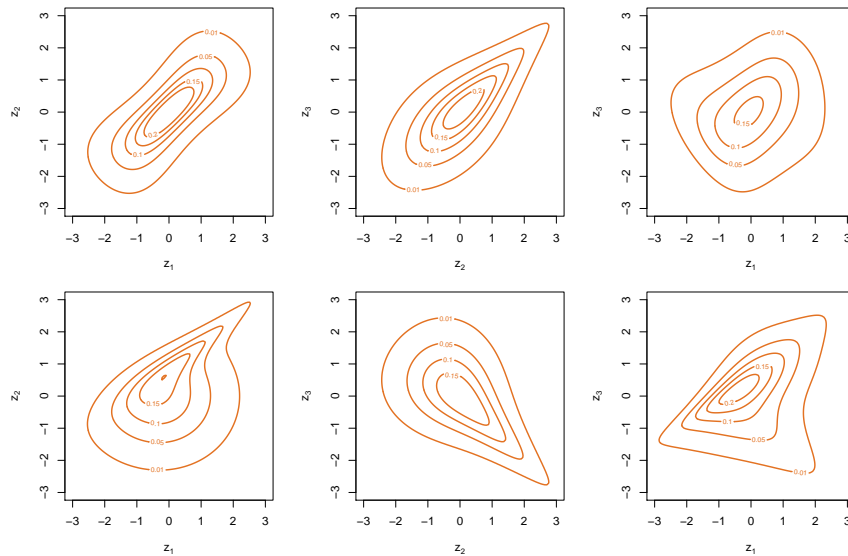


Figure 6: Contour plots of the bivariate margins c_{12} , c_{23} and c_{13} . Top row: Scenario 6. Bottom row: Scenario 7.

at all. Further, the non-exchangeable nature of the Tawn copula is noticeable both in the three- and the two-dimensional contour plots (cf. Figure 6, bottom row).

Note that even for the rather bent examples in this section the shape of the bivariate marginal contour plots resembles what we see in the three-dimensional plots. Thus, all con-

sidered simplified vines share the property that the mere knowledge of the three bivariate margins already provides a fairly good idea of the shape of the contours of the three-dimensional copula density.

4 Visualization of non-simplified vines

Having seen several examples of visualized simplified vines we also aim to visually explore the meaning of the simplifying assumption. For this purpose we now present a series of contour plots of non-simplified vine copula densities and try to make out differences between those and the simplified vines from Section 3. In Section 4 we will consider the non-simplified vine copula specifications from Table 2.

sc.	p.	copula c_{12}				copula c_{23}			
		family	$\theta_{12}^{(1)}$	$\theta_{12}^{(2)}$	τ_{12}	family	$\theta_{23}^{(1)}$	$\theta_{23}^{(2)}$	τ_{23}
8	12	\mathcal{N}	0	–	0	\mathcal{N}	0	–	0
9	13	t	0.6	3	0.41	t	0.7	7	0.49
10	14	t	0.6	3	0.41	t	0.7	7	0.49
11	14	\mathcal{C}	–2	–	–0.50	\mathcal{C}	2	–	0.50
12	14	\mathcal{F}	8	–	0.60	\mathcal{F}	8	–	0.60
13	16	\mathcal{G}	1.5	–	0.33	t	0	2.5	0
14	17	BB8	6	0.95	0.69	\mathcal{G}^{270}	–3.5	–	–0.71

sc.	p.	copula $c_{13;2}$		
		family	$\theta_{13;2}^{(1)}(u_2)$	$\theta_{13;2}^{(2)}(u_2)$
8	12	\mathcal{N}	$0.9 \sin(2\pi u_2)$	–
9	13	t	$0.1 + 0.8u_2$	5
10	14	t	0.5	$5 + 2.95 \sin(8\pi u_2)$
11	14	\mathcal{C}	$9(-(u_2 - 0.5)^2 + 0.25)$	–
12	14	AMH *	$1 - \exp(-8u_2)$	–
13	16	\mathcal{F}	$3 \arctan(10(u_2 - 0.5))$	–
14	17	$\mathcal{T}_{(2)}/\mathcal{T}_{(2)}^{90}$	$4 \operatorname{sgn}(u_2 - 0.5) - 3 \operatorname{sgn}(u_2 - 0.5) \cos(8\pi u_2)$	$0.1 + 0.8u_2$

Table 2: Non-simplified vine copula specifications considered in Section 4.

*AMH stands for the Ali-Mikhail-Haq copula. For a definition we refer to Kumar (2010).

4.1 Non-simplified vines with elliptical pair-copulas

Gaussian vine with sinal conditional dependence function

In our first non-simplified example (Scenario 8 from Table 2) we set the two unconditional copulas c_{12} and c_{23} to the independence copula in order to isolate the effect of the dependence of the conditional copula $c_{13;2}$ on u_2 . We choose $c_{13;2}$ to be Gaussian with parameter function $\rho_{13;2}(u_2) = 0.9 \sin(2\pi u_2)$, i.e. one full period of a sinus curve with amplitude 0.9. Hence, for values of u_2 ranging between 0 and 0.5 the dependence is positive with Kendall's τ between 0 and 0.71 and negative for $0.5 < u_2 < 1$ (see also the top left panel of Figure 8). The shift from positive to negative dependence is clearly visible in the contour plots shown in the top

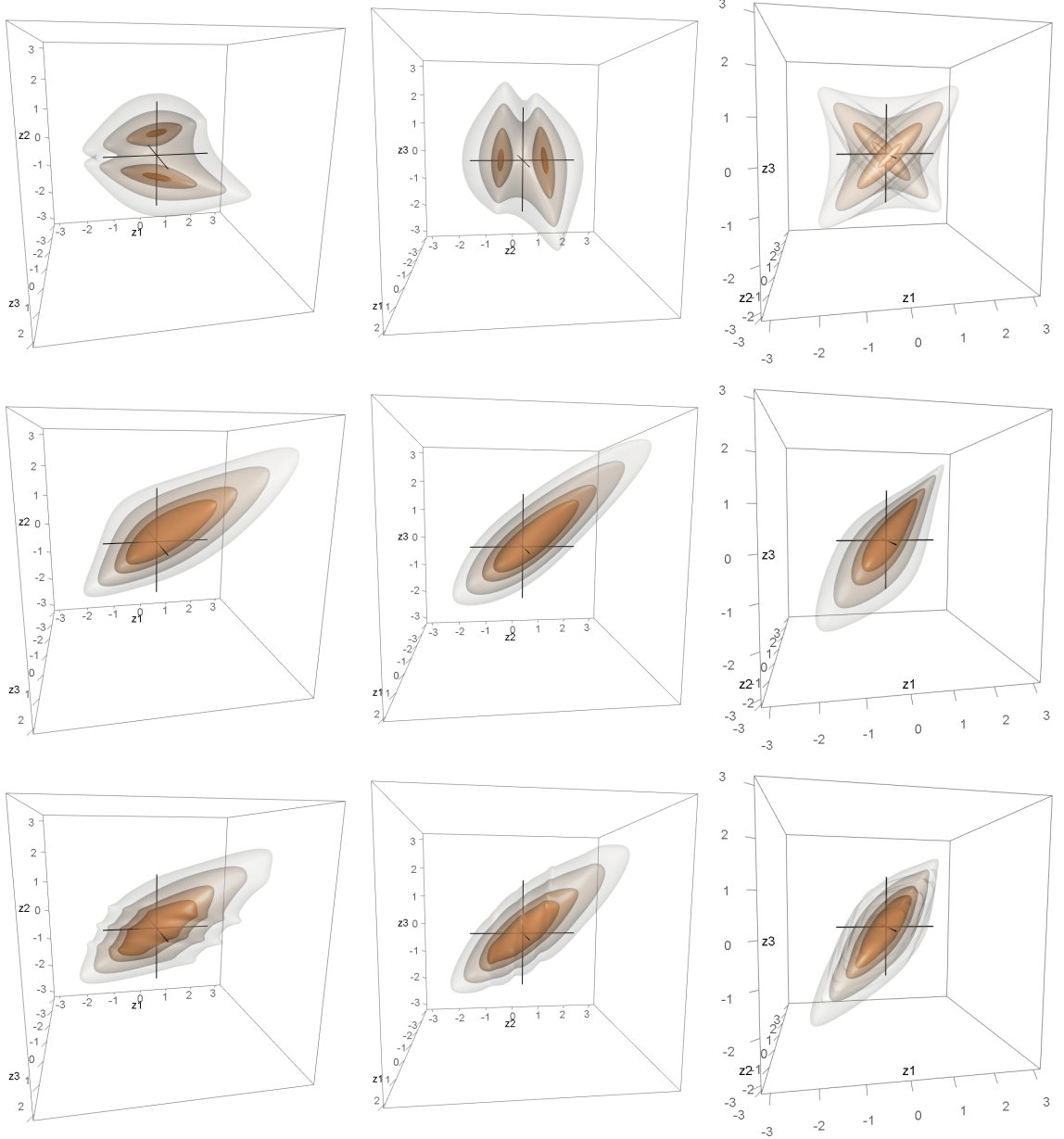


Figure 7: Top row (Scenario 8): Contours of the vine specified by $c_{12}: \mathcal{N}(0)$, $c_{23}: \mathcal{N}(0)$, $c_{13;2}: \mathcal{N}(\rho_{13;2}(u_2))$ with $\rho_{13;2}(u_2) = 0.9 \sin(2\pi u_2)$.

Middle row (Scenario 9): Contours of the vine specified by $c_{12}: t(0.6, 3)$, $c_{23}: t(0.7, 7)$, $c_{13;2}: t(\rho_{13;2}(u_2), 5)$ with $\rho_{13;2}(u_2) = 0.1 + 0.8u_2$.

Bottom row (Scenario 10): Contours of the vine specified by $c_{12}: t(0.6, 3)$, $c_{23}: t(0.7, 7)$, $c_{13;2}: t(0.5, \nu_{13;2}(u_2))$ with $\nu_{13;2}(u_2) = 5 + 2.95 \sin(8\pi u_2)$.

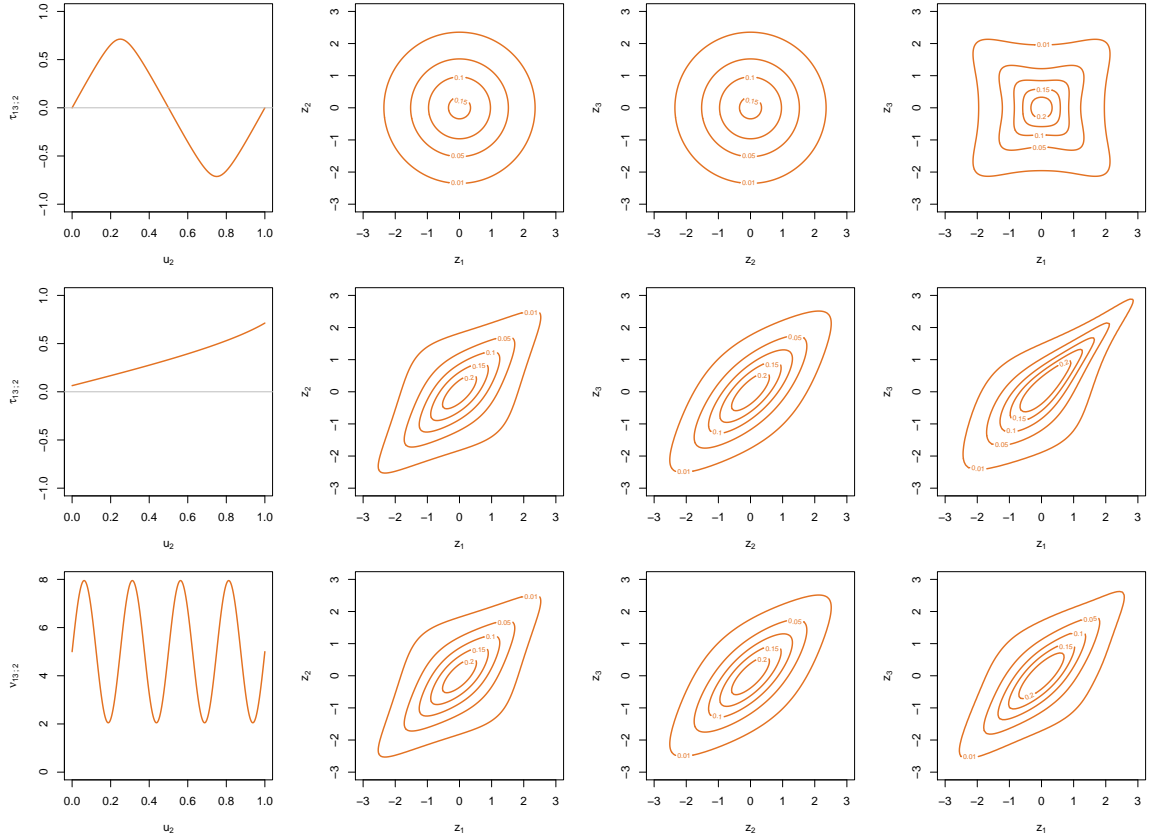


Figure 8: $\tau_{13;2}$ depending on u_2 and contour plots of the bivariate margins c_{12} , c_{23} and c_{13} . Top row: Scenario 8. Middle row: Scenario 9. Bottom row: Scenario 10. Note that the bottom left panel displays $\nu_{13;2}$ since $\tau_{13;2}$ is constant here.

row of Figure 7. We also observe that the resulting contour surfaces for higher levels are no longer connected and the density is bimodal. Further, from the numerically integrated contour plot of c_{13} in the top right panel of Figure 8 we conclude that marginally the strong positive and negative dependencies cancel each other out resulting in a bivariate marginal copula with almost no dependence, resembling a t copula with association of zero and low degrees of freedom.

t vine with linear conditional dependence function

For the non-simplified t vine we revisit the t vine of Section 3.1 and consider two different scenarios. In Scenarios 9 and 10 we let the values of the first and second parameter of the bivariate t copula $c_{13;2}$ depend on u_2 , respectively.

In Scenario 9 (cf. Table 2) the association parameter function of $c_{13;2}$ is linearly increasing in u_2 , ranging between 0.1 and 0.9 ($\tau_{13;2}$ between 0.06 and 0.71): $\rho_{13;2}(u_2) = 0.1 + 0.8u_2$ (see corresponding Kendall's τ values in the middle left panel of Figure 8). Thus, the average value of the association parameter is equal to 0.5, which is exactly $\rho_{13;2}$ from the corresponding simplified scenario. The contours in Figure 7 (middle row) still resemble those of the simplified t vine of Figure 1 (bottom row) on the first sight. However, taking a closer look one sees that the contour in the left plot has a noticeable bulge on the upper side and the one in the middle seems to be torn into the upper corner. The shape of the dependence function can be seen quite well in the right plot. In the lower corner, where the small values of z_2 (and therefore u_2) imply low association, the contour surfaces are much more round with less probability in the tails compared to their corresponding simplified versions. On the contrary, in the upper corner with respective large values of z_2 one clearly sees the high association, such that the surface seems to be drawn into the corner with a much sharper peak than its

simplified counterpart.

t vine with varying conditional degrees of freedom

It is also interesting to consider a non-simplified t vine where the degrees of freedom of the conditional copula depend on the conditioning variable. For this example (Scenario 10 from Table 2) we again revisit the t copula of Section 3.1 and let the degrees of freedom of $c_{13;2}$ vary periodically between 2.05 and 7.95 with an average value of 5 (which is equal to $\nu_{13;2}$ of the simplified Scenario 3): $\nu_{13;2}(u_2) = 5 + 2.95 \sin(8\pi u_2)$. These sinal waves can be seen in the contours of the density displayed in Figure 7 (bottom row). While the general shape of these contours is close to the ones from Figure 1 (bottom row), the density features bumps for certain values of the second variable. Interestingly, these bumps cannot be detected when looking at the two-dimensional contours in the bottom row of Figure 8. Since for a t copula the value of Kendall's τ does not depend on the degrees of freedom, $\tau_{13;2}$ is not depending on u_2 . Therefore, in the bottom left panel of Figure 8 we show a plot of $\nu_{13;2}$ instead.

In contrast to the simplified examples from Section 3, now the bivariate contour plots do no longer anticipate the three-dimensional object in a reasonable way. The sinal structure of Scenario 8 cannot be guessed from the plots in the top row of Figure 8. In fact, had we chosen $\rho_{13;2}(u_2) = -0.9 \sin(2\pi u_2)$, the copula density would have changed drastically (90 degree rotation along the z_2 -axis) while the bivariate margins would have stayed exactly the same. Further, we can observe that the first two margins of Scenario 9 and 10 are equal. However, the linearly increasing association parameter of Scenario 9 and the oscillating degrees of freedom of Scenario 10 are only visible in the three-dimensional contour plots (left and middle plots in the middle and bottom rows of Figure 7).

4.2 Non-simplified vines with Archimedean pair copulas

Clayton vine with quadratic conditional dependence function

We continue the example of a Clayton vine from Section 3.2, this time in a non-simplified form (see Scenario 11 in Table 2). We keep the dependencies of the unconditional pair-copulas as before at $\theta_{12} = -2$ and $\theta_{23} = 2$ and specify the parameter function as a downwardly open parabola taking only non-negative values: $\theta_{13;2}(u_2) = 9(-(u_2 - 0.5)^2 + 0.25)$. Its average value 1.5 is equal to $\theta_{13;2}$ of the simplified Clayton vine. The corresponding $\tau_{13;2}$ values range between 0 and 0.53 and take their maximum for $u_2 = 0.5$ (see the top left panel of Figure 10). The contours of the resulting density shown in the top row of Figure 9 look similar to those in the bottom row of Figure 3, but much more distorted. Especially the dependence between the first and third variables seems to change for different values of the second variable, which is an obvious indicator for a non-simplified vine. The contours of the bivariate margin c_{13} in the top right panel of Figure 10 also have a bent non-monotonic shape which is far from any of the standard parametric copulas that are only able to capture monotonic dependence. The bivariate contour plots of c_{12} and c_{23} (Figure 10, top row) suggest a smooth shape of the contours of the three-dimensional density such that one would not expect them to look as distorted as they do in the left and middle plots of the top row of Figure 9.

Three-dimensional Frank copula

As opposed to the Clayton copula, which can be expressed as a simplified vine (cf. Section 3.2), we now turn our attention to an Archimedean copula without this property, the three-dimensional Frank copula (with dependence parameter $\theta = 8$). Its non-simplified vine decomposition can be found as Scenario 12 in Table 2: The bivariate margins are again Frank copulas with the same dependence parameter θ . The copula of the conditioned variables $c_{13;2}$ is also Archimedean, belonging to the Ali-Mikhail-Haq (AMH) family with functional dependence parameter $\gamma_{13;2}(u_2) = 1 - \exp(-\theta u_2)$ (see Kumar (2010) and Spanhel and Kurz

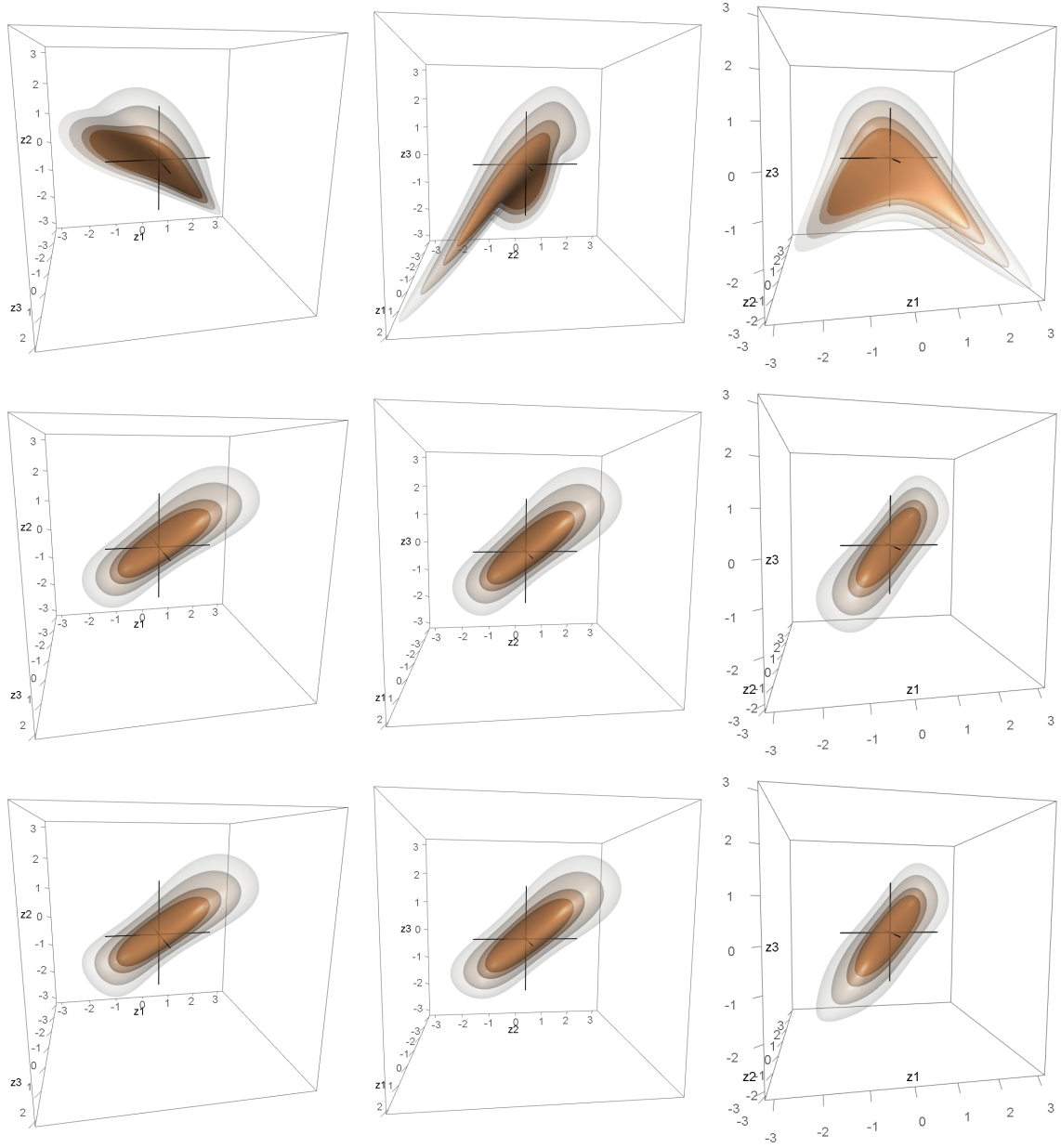


Figure 9: Top row (Scenario 11): Contours of the vine specified by c_{12} : $\mathcal{C}^{90}(-2)$, c_{23} : $\mathcal{C}(2)$, $c_{13;2}$: $\mathcal{C}(\theta_{13;2}(u_2))$ with $\theta_{13;2}(u_2) = 9(-(u_2 - 0.5)^2 + 0.25)$.
Middle row (Scenario 12): Contours of the vine specified by c_{12} : $\mathcal{F}(8)$, c_{23} : $\mathcal{F}(8)$, $c_{13;2}$: $\text{AMH}(\gamma_{13;2}(u_2))$ with $\gamma_{13;2}(u_2) = 1 - \exp(-8u_2)$.
Bottom row: Contours of the simplified vine approximation of Scenario 12.

(2015)). The corresponding τ values displayed in the middle left panel of Figure 10 show that the non-simplifiedness is not very pronounced. The strength of dependence is almost constant with the exception of small τ values for $u_2 < 0.2$. The contours depicted in the middle row of Figure 9 exhibit the typical bone shape known from the two-dimensional contour plots of bivariate Frank copulas such as those shown in the middle row of Figure 10. In order to assess how severe of a restriction the simplifying assumption would impose for modeling data generated by a Frank copula, we also present in the bottom row of Figure 9 and Figure 10 the three- and two-dimensional contours of a simplified vine approximation of the Frank copula, respectively. A simplified vine approximation is chosen such that the unconditional bivariate margins c_{12} and c_{23} are equal to the true margins and $c_{13;2}(\cdot, \cdot)$ equals the partial copula minimizing the Kullback-Leibler divergence to the conditional copula $c_{13;2}(\cdot, \cdot; u_2)$

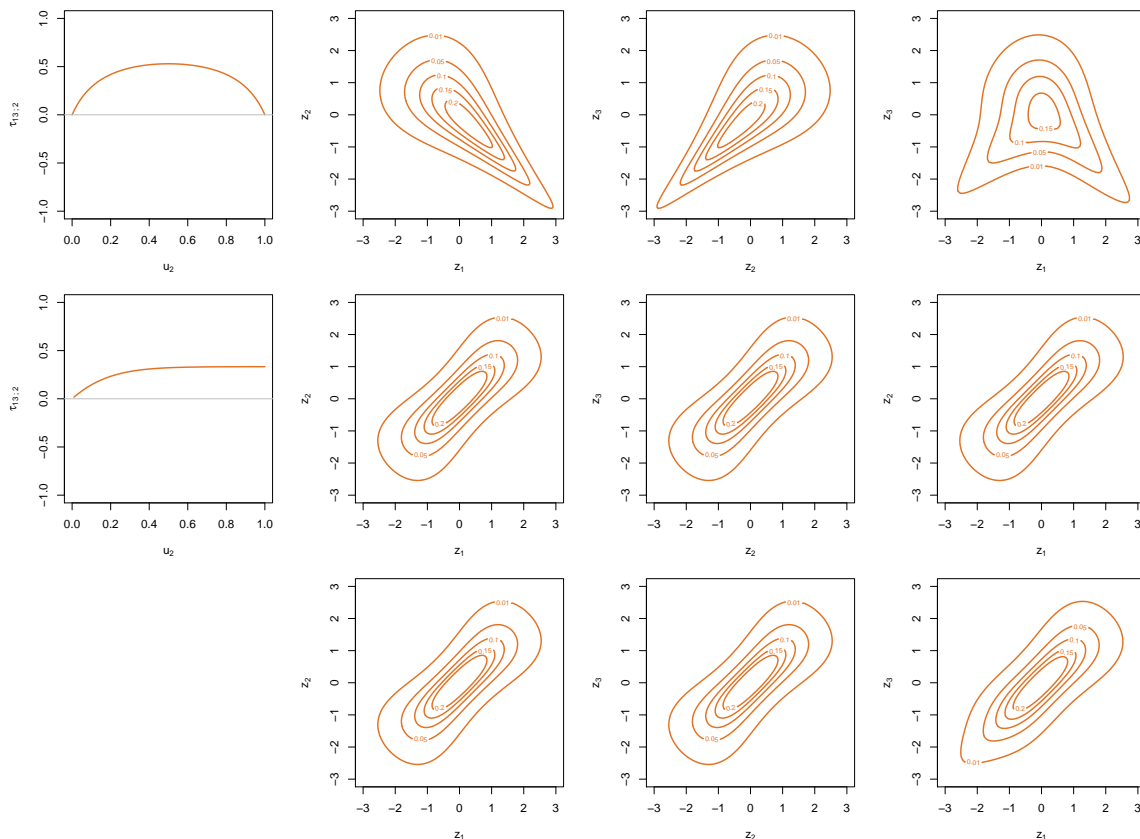


Figure 10: $\tau_{13;2}$ depending on u_2 and contour plots of the bivariate margins c_{12} , c_{23} and c_{13} . Top row: Scenario 11. Middle row: Scenario 12. Bottom row: simplified vine approximation of Scenario 12.

(for details see [Spanhel and Kurz \(2015\)](#)). The visual difference between the Frank copula and its simplified vine approximation seems almost negligible. Only from the angle where the dependence between the first and third variable is visible the two contour plots can be distinguished (see the right plots of the middle and bottom row of [Figure 9](#)). In the lower tail, where values of z_2 are small, the contours of the simplified vine approximation exhibit a higher dependence than the Frank copula, whose contours are more round implying less dependence. This is in line with what we would expect since the dependence function of $c_{13;2}$ of the non-simplified vine is decreasing for u_2 going to 0, while the dependence of $c_{13;2}$ of the simplified vine approximation is constant at $\tau_{13;2} = 0.28$.

4.3 Mixed non-simplified vine specifications

Mixed non-simplified vine with low dependence

As in the section about simplified vines we also consider non-simplified vines where the pair-copulas come from different parametric families. We highlight two scenarios, one with rather low and one with high dependence. For the low dependence scenario (Scenario 13 from [Table 2](#)) we choose c_{12} to be a Gumbel copula with parameter $\theta_{12} = 1.5$, c_{23} as a t copula with $\rho_{23} = 0$ and 2.5 degrees of freedom and $c_{13;2}$ as a Frank copula with parameter function $\theta_{13;2}(u_2) = 3 \arctan(10(u_2 - 0.5))$, implying negative dependence for $u_2 < 0.5$ and positive dependence for $u_2 > 0.5$ with absolute τ values smaller than 0.4 (compare [Figure 12](#), top left panel). The low dependence of the copula density is clearly visible from the contour plots in [Figure 11](#). However, the surfaces look quite crumpled with lots of irregular bumps and deformations. Moreover, it is eye-catching that in this scenario we only observe three contour surfaces. The inner surface is missing since the density only take values between 0

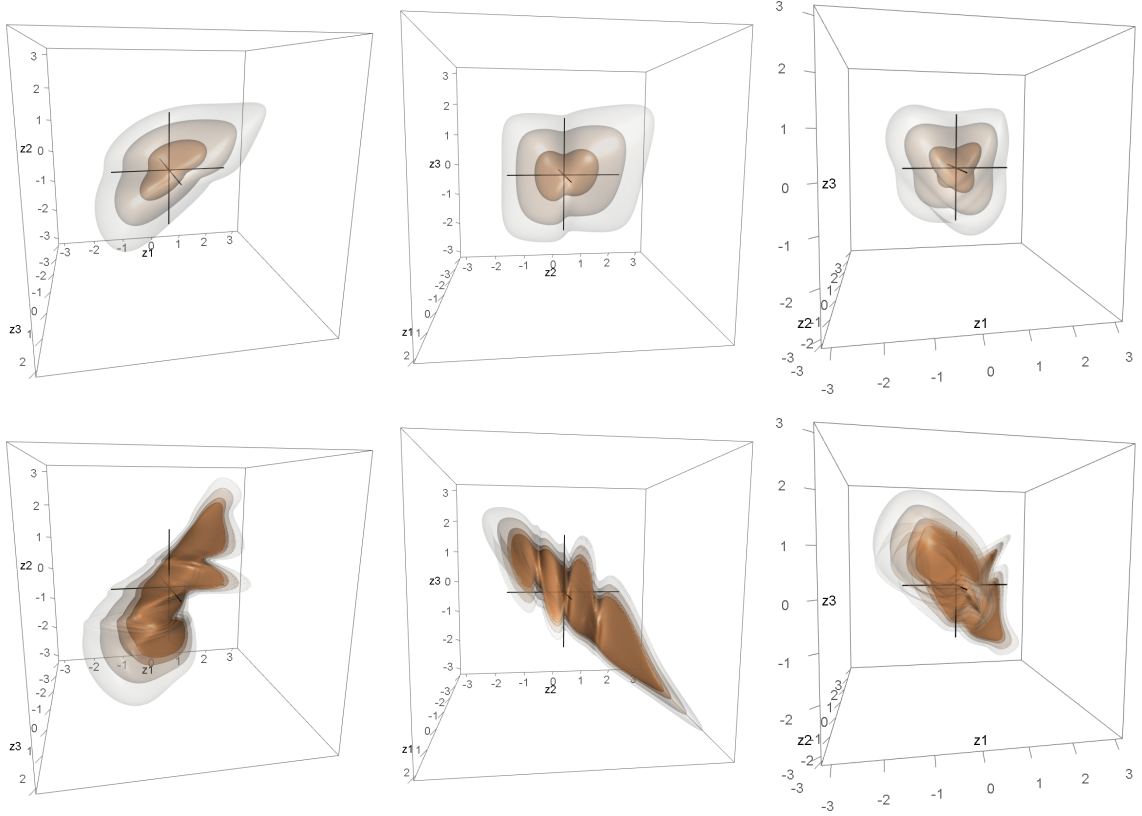


Figure 11: Top row (Scenario 13): Contours of the vine specified by c_{12} : $\mathcal{G}(1.5)$, c_{23} : $t(0, 2.5)$, $c_{13;2}$: $\mathcal{F}(\theta_{13;2}(u_2))$ with $\theta_{13;2}(u_2) = 3 \arctan(10(u_2 - 0.5))$. Bottom row (Scenario 14): Contours of the vine specified by c_{12} : $\text{BB8}(6, 0.95)$, c_{23} : $\mathcal{G}^{270}(-3.5)$, $c_{13;2}$: $\mathcal{T}_{(2)}/\mathcal{T}_{(2)}^{90}(\theta_{13;2}^{(1)}(u_2), \theta_{13;2}^{(2)}(u_2))$ with $\theta_{13;2}^{(1)}(u_2) = 4 \text{sgn}(u_2 - 0.5) - 3 \text{sgn}(u_2 - 0.5) \cos(8\pi u_2)$ and $\theta_{13;2}^{(2)}(u_2) = 0.1 + 0.8u_2$.

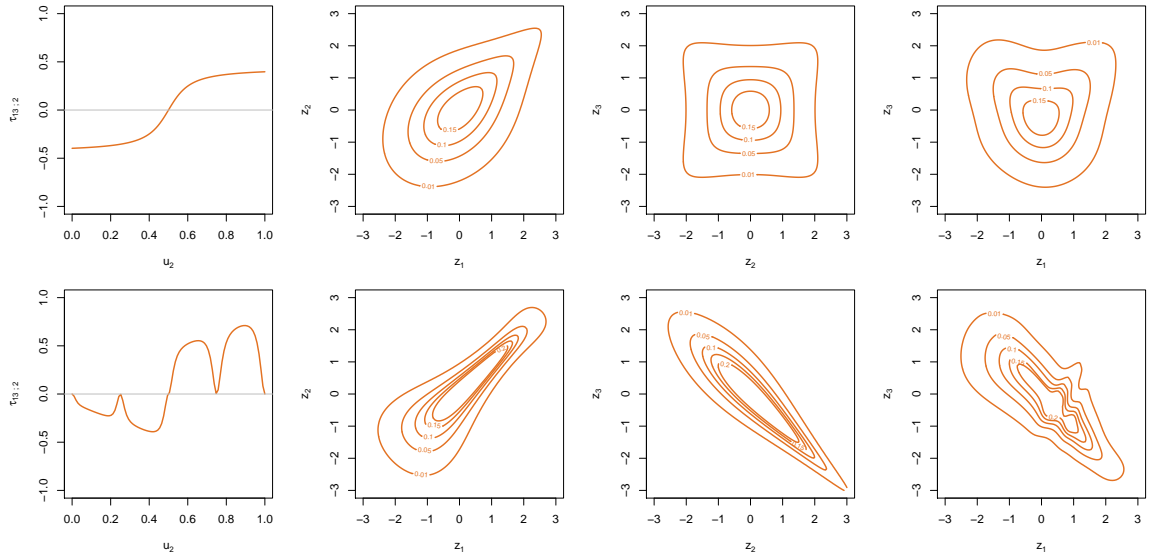


Figure 12: $\tau_{13;2}$ depending on u_2 and contour plots of the bivariate margins c_{12} , c_{23} and c_{13} . Top row: Scenario 13. Bottom row: Scenario 14.

and 0.101 but the level of the inner surface is 0.11. Further, due to the low dependence we cannot detect any corner with extraordinarily high probability mass.

Mixed non-simplified vine with high dependence

The last example we consider is Scenario 14 (see [Table 2](#)). It is more extreme featuring pair-copulas with high dependence and more involved functions for the parameters of $c_{13;2}$. We specify c_{12} as a BB8 copula with parameters $\theta_{12} = (6, 0.95)'$, c_{23} as a Gumbel copula rotated by 270 degrees with $\theta_{23} = -3.5$ and $c_{13;2}$ as a Tawn Type 2 copula with both parameters depending on u_2 via the functions $\theta_{13;2}^{(1)}(u_2) = 4 \operatorname{sgn}(u_2 - 0.5) - 3 \operatorname{sgn}(u_2 - 0.5) \cos(8\pi u_2)$ and $\theta_{13;2}^{(2)}(u_2) = 0.1 + 0.8u_2$. The corresponding τ values ranging between -0.39 and 0.71 are shown in the bottom left panel of [Figure 12](#). For the values of $u_2 < 0.5$ that imply negative dependence we use the 90 degree rotated version of the Tawn type 2 copula. [Figure 11](#) (bottom row) displays the contour plots of the resulting density. This is by far the most contorted density. The four peaks of the $\tau_{13;2}$ function are also clearly visible as bumps in the three-dimensional contour plots. Of course, one can argue about how realistic it is to assume that real data follows such a distribution but it illustrates the variety of densities which can be modeled using non-simplified parametric vines.

Considering Scenario 13 we can state that again the bivariate marginal contours do not really anticipate the complex shape of the corresponding three-dimensional object. In Scenario 14 this observation is even more pronounced: the contour plots of c_{12} and c_{23} in [Figure 12](#) look perfectly smooth and regular and do not at all suggest the extremely twisted and contorted structure which can be seen in the bottom left and middle panel of [Figure 11](#).

5 Application to simulated and real data

In this section we want to investigate if the contour plots can help to decide whether a simplified or a non-simplified specification for given data is needed. For this purpose, we at first consider simulated data, where we know the true underlying distribution, and afterwards apply the method to real data.

5.1 Simulation study

For the simulated data example, we revisit the mixed non-simplified vine with low dependence (Scenario 13 from [Section 4.3](#)). We generate a sample of size $N = 3000$ from this model and transform the margins to be standard normal in order to make results comparable to the ones from the previous sections. For this transformed data sample, we perform a standard kernel density estimation with the function `kde` from the R package `ks` ([Duong \(2016\)](#)) using Gaussian kernels. Note that using this method we only get approximately standard normal margins. The contours of the resulting estimated densities, which are shown in the top row of [Figure 13](#), are very close to those of the true underlying density (cf. [Figure 11](#), top row). Only the innermost contour surface is smaller because the peaks of the density tend to get averaged out by kernel density estimation. [Figure 14](#) (top row) displays the contours of the corresponding kernel density estimated bivariate margins, which are again close to the true ones in the top row of [Figure 12](#).

The idea is now to compare these contour plots to those of estimated simplified and non-simplified vine densities. We use `RVineStructureSelect` (from `VineCopula`) to fit a simplified vine and `gamVineStructureSelect` (from `gamCopula`) to fit a non-simplified vine. Both algorithms estimate the same unconditional copulas: c_{12} is fitted as a Gumbel copula with parameter $\hat{\theta}_{12} = 1.47$ (implying $\hat{\tau}_{12} = 0.32$) and c_{23} as a t copula with $\hat{\rho}_{23} = 0.02$ and $\hat{\nu}_{23} = 2.54$ degrees of freedom ($\hat{\tau}_{23} = 0.02$). In the simplified setting $c_{13;2}$ is estimated as a Tawn Type 1 copula rotated by 270 degrees with $\hat{\theta}_{13;2} = (-1.14, 0.21)'$, such that $\hat{\tau}_{13;2} = -0.05$. The corresponding contours are shown in the middle row of [Figure 13](#). They seem to be a smoothed version of the kernel estimated density contours. While the general strengths of dependence are represented pretty well, the simplified vine approximation does

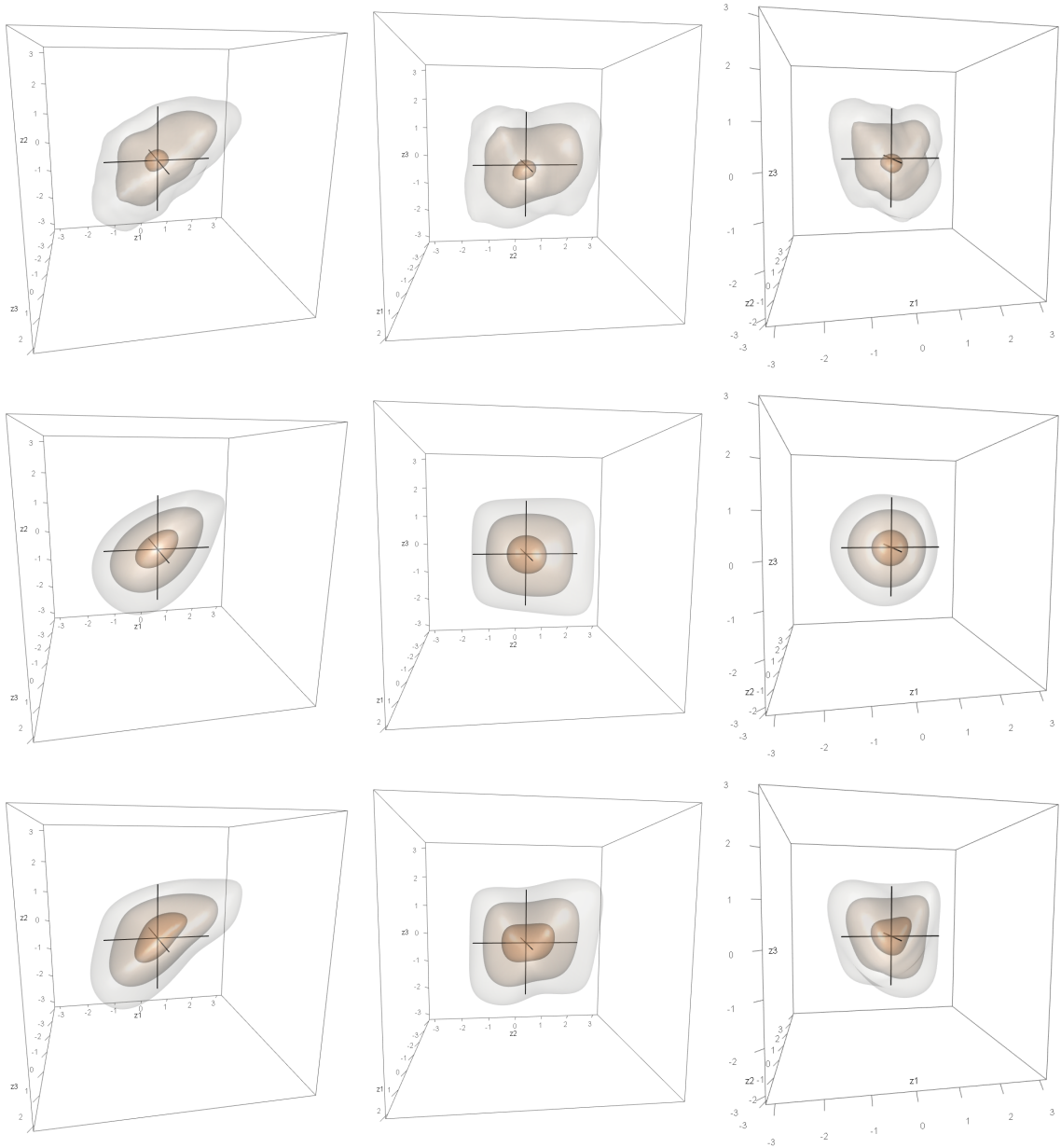


Figure 13: Top row: Contours of the density estimated via three-dimensional kernel density estimation.

Middle row: Contours of the simplified vine specified by c_{12} : $\mathcal{G}(1.47)$, c_{23} : $t(0.02, 2.54)$, $c_{13;2}$: $\mathcal{T}_{(1)}^{270}(-1.14, 0.21)$.

Bottom row: Contours of the non-simplified vine specified by c_{12} : $\mathcal{G}(1.47)$, c_{23} : $t(0.02, 2.54)$, $c_{13;2}$: $\mathcal{N}(\hat{\rho}_{13;2}(u_2))$.

not feature the bumps and dents of the kernel density estimated surfaces. A look at the contours of the bivariate margins in the middle row of [Figure 14](#) reveals that the densities of the explicitly modeled margins c_{12} and c_{23} are fitted very well (the true copula families are chosen and the estimated parameters 1.47 and 0.02 are close to the true values 1.5 and 0). However, the contours of the implicitly defined margin c_{13} are far from the ones of the kernel density estimate. This is another indicator for an insufficient fit resulting from the simplifying assumption, which is in this case too restrictive.

We now investigate whether these deficiencies can be remedied by fitting a non-simplified vine to the simulated data. The algorithm `gamVineStructureSelect` estimates the copula $c_{13;2}$ to be Gaussian with parameter function $\hat{\rho}_{13;2}(u_2)$ depending on u_2 via the functional

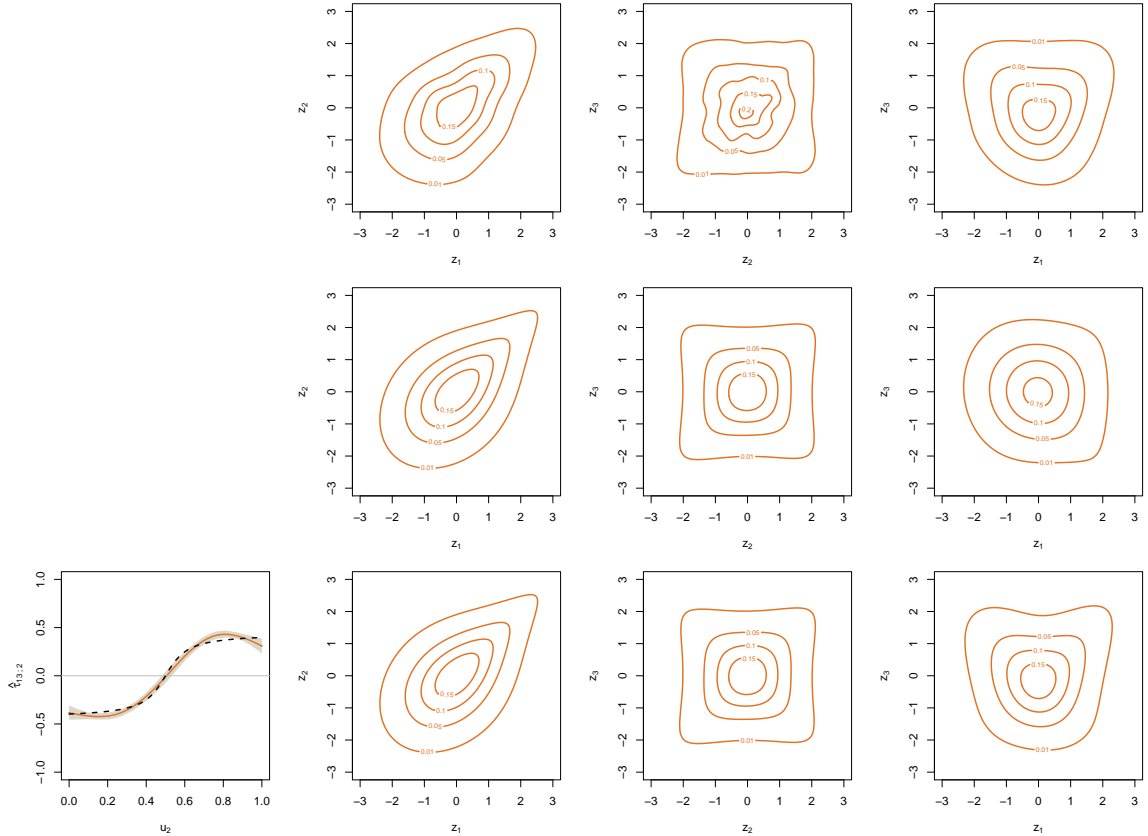


Figure 14: Contour plots of the bivariate margins c_{12} , c_{23} and c_{13} and $\hat{\tau}_{13;2}$ depending on u_2 . Top row: kernel density estimation. Middle row: estimated simplified vine. Bottom row: estimated non-simplified vine.

form displayed in the bottom left panel of [Figure 14](#) (in terms of $\hat{\tau}_{13;2}$), together with its bootstrapped 95%-confidence intervals (gray) and the true $\tau_{13;2}$ curve (dashed line). The τ -values range between -0.36 and 0.38 with negative values for $u_2 < 0.5$ such that the estimated function is quite close to the true underlying τ -function. Even though the wrong copula family is chosen for $c_{13;2}$ (Gaussian instead of Frank) the contours of the resulting non-simplified vine in [Figure 13](#) (bottom row) are very similar to the kernel estimated ones and fit their shape considerably better than the estimated simplified vine. Also, the contours of the bivariate margin c_{13} in the bottom right panel of [Figure 14](#) now provide a much better fit. Hence, we can conclude that in this example we are able to visually detect the non-simplifiedness of the true distribution.

5.2 Real data application

In the following section we want to apply this method to a real data example. We investigate the well-known `uranium` data set, which can be found in the R package `copula`. This data set consists of 655 chemical analyses from water samples from a river near Grand Junction, Colorado (USA). It contains the log-concentration of seven chemicals, where we will focus on the three elements cobalt (X_1), titanium (X_2) and scandium (X_3) that have already been examined regarding the simplifying assumption in [Acar et al. \(2012\)](#) and [Killiches et al. \(2015\)](#). In order to obtain copula data we first apply the probability integral transform to the data using the empirical marginal distribution functions, i.e. the observations x_{ji} , $j = 1, 2, 3$, $i = 1, \dots, N$, are transformed via the rank transformation

$$u_{ji} = \frac{1}{N+1} \sum_{k=1}^N 1_{\{x_{jk} \leq x_{ji}\}},$$

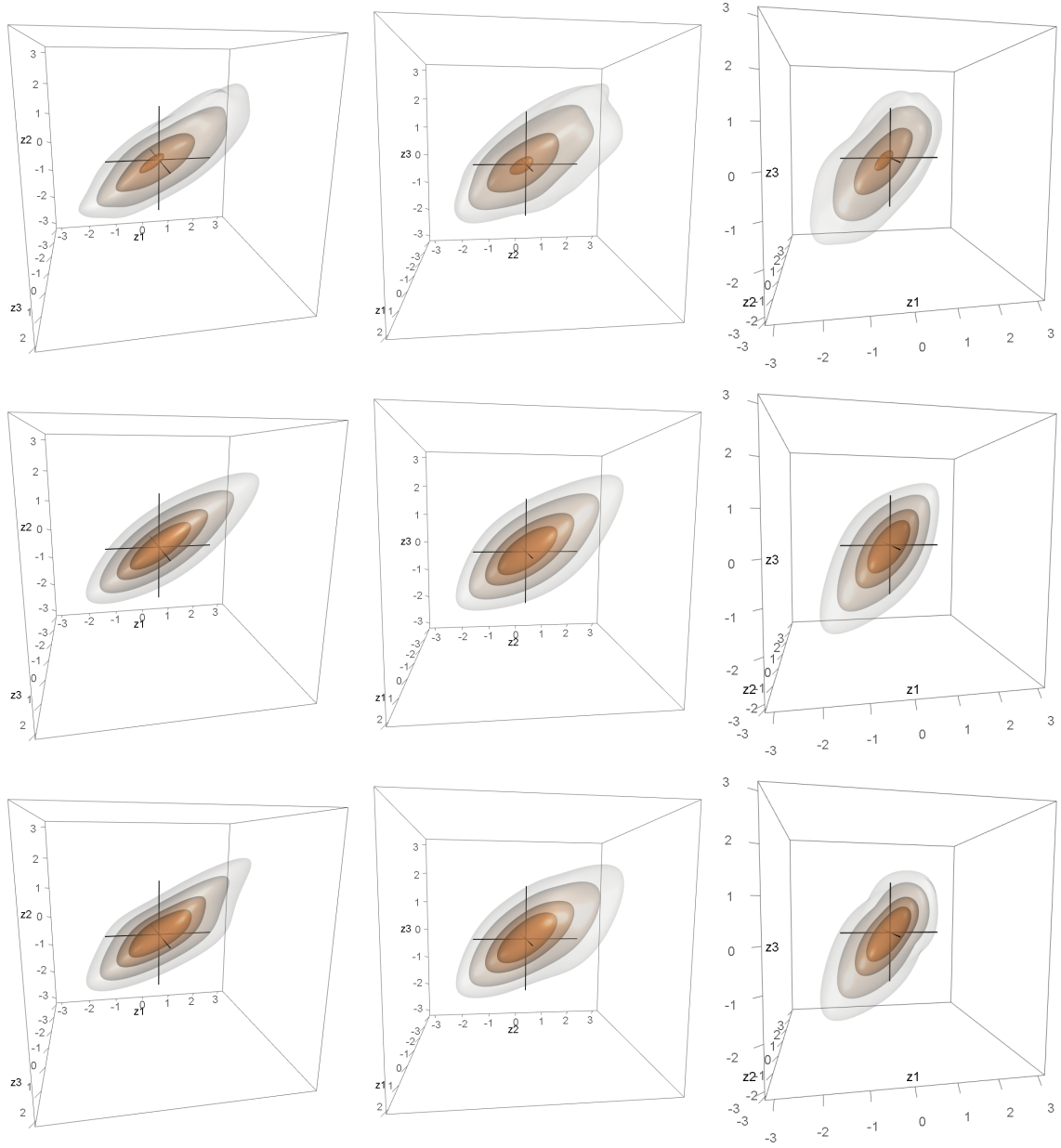


Figure 15: Top row: Contours of the density estimated via three-dimensional kernel density estimation.

Middle row: Contours of the simplified vine specified by c_{12} : $t(0.53, 8.03)$, c_{23} : $t(0.43, 5.93)$, $c_{13;2}$: $t(0.08, 5.65)$.

Bottom row: Contours of the non-simplified vine specified by c_{12} : $t(0.53, 8.03)$, c_{23} : $t(0.43, 5.93)$, $c_{13;2}$: $t(\hat{\rho}_{13;2}(u_2), 6.69)$.

where $1_{\{\cdot\}}$ is the indicator function. Then, we transform the data to have standard normal margins in accordance to the previous examples.

We now want to take a look at the “true” model and perform a kernel density estimation. In the top rows of [Figure 15](#) and [Figure 16](#) the results of the three- and two-dimensional kernel density estimations are displayed, respectively. The three variables seem to be positively dependent. A few bumps and dents are noticeable. Next we explore how well estimated simplified and non-simplified vines fit the data.

Using `RVineStructureSelect` we obtain the following simplified vine: c_{12} is a t copula with $\hat{\rho}_{12} = 0.74$ and $\hat{\nu}_{12} = 8.03$ ($\hat{\tau}_{12} = 0.53$), c_{23} is a t copula with $\hat{\rho}_{23} = 0.63$ and $\hat{\nu}_{23} = 5.93$ ($\hat{\tau}_{23} = 0.43$) and $c_{13;2}$ is a t copula with $\hat{\rho}_{13;2} = 0.08$ and $\hat{\nu}_{13;2} = 5.65$ ($\hat{\tau}_{13;2} = 0.05$). This t

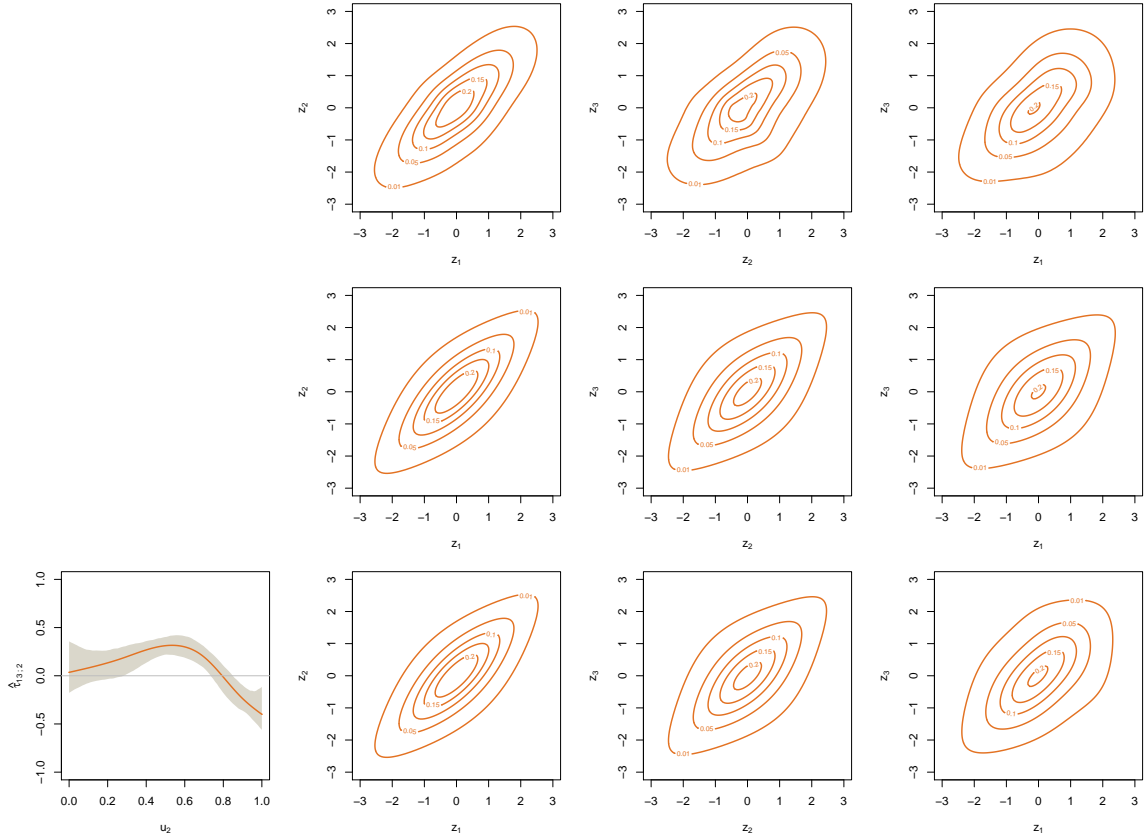


Figure 16: Contour plots of the bivariate margins c_{12} , c_{23} and c_{13} and $\hat{\tau}_{13;2}$ depending on u_2 . Top row: kernel density estimation. Middle row: estimated simplified vine. Bottom row: estimated non-simplified vine.

vine and its bivariate margins are depicted in [Figure 15](#) (middle row) and [Figure 16](#) (middle row), respectively. Since all three degrees of freedom are of medium size we observe modest lower and upper tail dependence. Again, these contours resemble a smoothed version of the slightly bumpy kernel density estimated contour surfaces resulting in a rather unsatisfying fit of the data.

For the non-simplified vine, the estimates of c_{12} and c_{23} are the same as for the simplified one. The third pair-copula $c_{13;2}$ is still a t copula but now with $\hat{\nu}_{13;2} = 6.69$ degrees of freedom and an association parameter depending on u_2 . We show the relationship between u_2 and $\hat{\tau}_{13;2}$ in the bottom left panel of [Figure 16](#) (again with its bootstrapped 95%-confidence intervals). One can see that we have small positive values of Kendall's τ for $u_2 \leq 0.8$ and negative dependence for the remaining values of u_2 . Although only the parameters of the copula $c_{13;2}$ are different compared to the simplified vine, the shapes of the contour surfaces display some interesting changes: Especially in the left and the bottom right panel of [Figure 15](#), we see that the diamond-shaped contours from [Figure 15](#) (middle row) have developed several dents. While the contour plots of c_{12} and c_{23} are the same as before, the one of c_{13} exhibits some differences being no longer diamond-shaped.

Comparing these contours to the ones from the top rows of [Figure 15](#) and [Figure 16](#) we see that the non-simplified vine is able to capture the behavior of the data quite well. The most noticeable bumps and dents are reproduced and the bivariate contours resemble the kernel density estimated ones. Thus, we come to the same conclusions as [Acar et al. \(2012\)](#) and [Killiches et al. \(2015\)](#), namely that the vine copula decomposition of this three-dimensional data set is of the non-simplified form.

6 Conclusion

In this paper we have looked at the contour surfaces of several three-dimensional simplified and non-simplified vine copulas. The flexibility of simplified vines in comparison to standard elliptical and Archimedean copulas has been demonstrated. Using the 12 different one- and two-parametric bivariate pair-copula families currently implemented in `VineCopula` for the construction of a simplified vine, the shape of the resulting contour surfaces may deviate considerably from the well-known ellipsoid-shaped contours of a Gaussian distribution. Considering non-simplified vines facilitates the modeling of even more irregular contour shapes exhibiting twists, bumps and altering dependence patterns. In our examples we have observed that contemplating three-dimensional contour surfaces gives more insight into the trivariate dependence structure than only looking at the two-dimensional marginal contour lines. While the consideration of the three bivariate marginal contour plots already gives a good impression of the shape of the three-dimensional object for simplified vines, one might be surprised how twisted and contorted some non-simplified three-dimensional densities look like if one had only seen the smooth bivariate contour plots. In simulated and real data applications we have seen that non-simplified vines are able to fit data with complex dependencies very well. Having said that, we have also observed that the estimated simplified vines still capture the main features of the data providing a more smooth fit. Thus, for practical applications, especially in higher dimensions (when the number as well as the dimension of the parameter functions increases, which causes numerical intractability) it might be preferable to use simplified vines. Thereby overfitting might be avoided while the main properties of the data such as correlations and tail behavior are still well represented.

Acknowledgment

The first author is thankful for the support from Allianz Deutschland AG, the third author is supported by the German Research Foundation (DFG grant GZ 86/4-1).

References

- Aas, K., Czado, C., Frigessi, A., and Bakken, H. (2009). Pair-copula constructions of multiple dependence. *Insurance, Mathematics and Economics*, 44:182–198.
- Acar, E. F., Genest, C., and Nešlehová, J. (2012). Beyond simplified pair-copula constructions. *Journal of Multivariate Analysis*, 110:74–90.
- Basel Committee on Banking Supervision (2009). Consultative document: International framework for liquidity risk measurement, standards and monitoring.
- Bedford, T. and Cooke, R. M. (2002). Vines: A new graphical model for dependent random variables. *Annals of Statistics*, pages 1031–1068.
- Brechmann, E., Czado, C., and Paterlini, S. (2014). Flexible dependence modeling of operational risk losses and its impact on total capital requirements. *Journal of Banking & Finance*, 40:271–285.
- Brechmann, E. C. and Czado, C. (2013). Risk management with high-dimensional vine copulas: An analysis of the Euro Stoxx 50. *Statistics & Risk Modeling*, 30(4):307–342.
- Demarta, S. and McNeil, A. J. (2005). The t copula and related copulas. *International statistical review*, 73(1):111–129.

- Dißmann, J., Brechmann, E. C., Czado, C., and Kurowicka, D. (2013). Selecting and estimating regular vine copulae and application to financial returns. *Computational Statistics & Data Analysis*, 59:52–69.
- Duong, T. (2016). *ks: Kernel Smoothing*. R package version 1.10.1.
- Erhardt, T. M., Czado, C., and Schepsmeier, U. (2015a). R-vine models for spatial time series with an application to daily mean temperature. *Biometrics*.
- Erhardt, T. M., Czado, C., and Schepsmeier, U. (2015b). Spatial composite likelihood inference using local C-vines. *Journal of Multivariate Analysis*, 138:74–88.
- European Parliament and European Council (2009). Directive 2009/138/EC of the European Parliament and of the Council of 25 November 2009 on the taking-up and pursuit of the business of Insurance and Reinsurance (Solvency II) (recast).
- Haff, I. H., Aas, K., and Frigessi, A. (2010). On the simplified pair-copula construction – simply useful or too simplistic? *Journal of Multivariate Analysis*, 101(5):1296–1310.
- Hofert, M., Kojadinovic, I., Maechler, M., and Yan, J. (2015). *copula: Multivariate Dependence with Copulas*. R package version 0.999-14.
- Joe, H. (1997). *Multivariate models and multivariate dependence concepts*. CRC Press.
- Killiches, M. and Czado, C. (2015). Block-maxima of vines. In D. Dey and J. Yan. (Eds.), *Extreme Value Modelling and Risk Analysis: Methods and Applications*. Chapman & Hall/CRC Press.
- Killiches, M., Kraus, D., and Czado, C. (2015). Model distances for vine copulas in high dimensions with application to testing the simplifying assumption. *arXiv preprint arXiv:1510.03671*.
- Kraus, D. and Czado, C. (2015). D-vine Copula Based Quantile Regression. *arXiv preprint arXiv:1510.04161*.
- Kumar, P. (2010). Probability distributions and estimation of Ali-Mikhail-Haq copula. *Applied Mathematical Sciences*, 4(14):657–666.
- Kurowicka, D. and Cooke, R. M. (2006). *Uncertainty analysis with high dimensional dependence modelling*. John Wiley & Sons.
- Maya, L., Albeiro, R., Gomez-Gonzalez, J. E., and Melo Velandia, L. F. (2015). Latin american exchange rate dependencies: A regular vine copula approach. *Contemporary Economic Policy*, 33(3):535–549.
- Nagler, T. and Czado, C. (2015). Evading the curse of dimensionality in multivariate kernel density estimation with simplified vines. *arXiv preprint arXiv:1503.03305*.
- Nelsen, R. (2006). An introduction to copulas, 2nd. *New York: Springer Science Business Media*.
- Panagiotelis, A., Czado, C., and Joe, H. (2012). Pair copula constructions for multivariate discrete data. *Journal of the American Statistical Association*, 107(499):1063–1072.
- Schepsmeier, U., Stöber, J., Brechmann, E. C., Gräler, B., Nagler, T., and Erhardt, T. (2015). *VineCopula: Statistical inference of vine copulas*. R package version 1.6.
- Sklar, A. (1959). Fonctions de répartition à n dimensions et leurs marges. *Publ. Inst. Stat. Univ. Paris*, 8:229–231.

- Spanhel, F. and Kurz, M. S. (2015). Simplified vine copula models: Approximations based on the simplifying assumption. *arXiv preprint arXiv:1510.06971*.
- Stöber, J. and Czado, C. (2012). Pair copula constructions. In J.-F. Mai and M. Scherer (2012), *Simulating Copulas: Stochastic Models, Sampling Algorithms, and Applications*. World Scientific.
- Stöber, J., Joe, H., and Czado, C. (2013). Simplified pair copula constructions limitations and extensions. *Journal of Multivariate Analysis*, 119:101–118.
- Vatter, T. (2015). *gamCopula: Generalized Additive Models for Bivariate Conditional Dependence Structures and Vine Copulas*. R package version 0.0-1.
- Vatter, T. and Nagler, T. (2015). Generalized additive models for pair-copula constructions. Working paper.